



Battery system architecture and dimensioning for urban track system

Lappeenranta–Lahti University of Technology LUT

Bachelor's Programme in Electrical Engineering (Double Degree, in co-operation with Hebei University of Technology)

2025

XINYU HOU

Examiner(s): Associate professor Lassi Aarniovuori

Jussi Niemioja (UDT)

ABSTRACT

Lappeenranta–Lahti University of Technology LUT

LUT School of Energy Systems

Electrical Engineering

In co-operation with partner university: HEBEI University of Technology

XINYU HOU

Battery system architecture and dimensioning for urban track system

Bachelor's thesis

2025

41 pages, 18 figures, 13 tables and 0 appendices

Examiner(s): Associate professor Lassi Aarniovuori, Jussi Niemioja(UDT)

Keywords: Dual-battery system; Voltage conversion; Decentralization of BMS systems; Regenerative braking

With the acceleration of urbanization, urban traffic congestion and environmental pollution problems have become increasingly prominent. This paper proposes a dual-battery system architecture suitable for urban rail transit, which consists of a drive battery and an auxiliary battery. Through functional division and good optimization, the system efficiency and reliability are improved. The drive battery powers the cabin drive unit and charges the auxiliary battery. The auxiliary battery provides a stable 24V voltage for the traction control system and other auxiliary equipment. Through Simulink modeling and simulation, the system achieves a stable 24V output at a 60-100V input. The battery life is extended by controlling the battery power and the battery utilization is improved through regenerative braking technology.

Table of contents

Abstract

| | | |
|-------|---|----|
| 1 | Introduction | 1 |
| 1.1 | Background | 1 |
| 1.2 | Research status of battery technology at home and abroad | 2 |
| 1.3 | Dual-battery System Overview | 3 |
| 1.4 | The analysis to the advantages and disadvantages to the dual-battery system | 4 |
| 1.4.1 | The advantages of the dual-battery system..... | 4 |
| 1.4.2 | The disadvantages of the dual-battery system | 5 |
| 1.5 | Research targets | 5 |
| 2 | Method..... | 7 |
| 2.1 | Basic framework design of dual battery system | 7 |
| 2.2 | Auxiliary battery | 8 |
| 2.2.1 | Auxiliary battery design..... | 8 |
| 2.2.2 | Calculation of auxiliary battery related parameters and selection of components..... | 8 |
| 2.3 | Drive battery..... | 10 |
| 2.3.1 | Drive battery design..... | 10 |
| 2.3.2 | The calculation of drive battery related parameters and components selection to the drive battery | 10 |
| 2.4 | Voltage conversion circuit | 13 |
| 2.4.1 | Voltage conversion circuit design..... | 13 |
| 2.4.2 | Parameter calculation and selection of conversion circuit components | 15 |
| 2.5 | Optimization to the dual-battery system | 18 |
| 2.5.1 | Auxiliary battery protection..... | 18 |
| 2.5.2 | Application of regenerative braking technology | 19 |
| 2.6 | The calculation to the time that the capsule can be operational without the drive battery..... | 22 |
| 2.7 | Environmental conditions to be considered | 22 |
| 2.7.1 | High temperature environment | 22 |

| | | |
|-------|---|----|
| 2.7.2 | Low temperature environment..... | 23 |
| 2.8 | Drive battery replacement scheme..... | 23 |
| 2.9 | Decentralization of BMS systems – analysis..... | 24 |
| 3 | Result..... | 26 |
| 3.1 | Auxiliary battery parameters and models..... | 26 |
| 3.2 | The time that the capsule can be operational without the drive battery..... | 26 |
| 3.3 | Drive battery parameters..... | 27 |
| 3.4 | Parameters and models of conversion circuit related components..... | 27 |
| 3.5 | Dual-battery system modeling and simulation..... | 29 |
| 4 | Conclusions..... | 33 |
| | References..... | 35 |

1 Introduction

1.1 Background

In the future, as urbanization continues to advance, air pollution will become more serious (Namrata et al. 2022, 1553–1563). The acceleration of industrialization and the surge in the number of cars brought about by urbanization have driven the emission of a large amount of harmful gases, especially automobile exhaust and industrial waste gas, leading to the continuous deterioration of air quality. This not only harms the health of residents, but also has a long-term impact on the ecosystem (Elmi et al. 2012, 619-624; Vallejo et al. 2023, e0291838–e0291838).

At the same time, the advancement of urbanization has also directly led to increasingly serious traffic congestion (Zhou et al. 2022, 1-9). With the continuous increase in urban population and the increasing economic activities, traffic demand has increased rapidly, and the existing transportation infrastructure has gradually been unable to meet the demand, resulting in road congestion and low travel efficiency (Huang et al. 2023, 592-614). Therefore, as urbanization continues to advance, cities in the future will face more severe challenges of air pollution and traffic congestion, which puts higher demands on the sustainable development of cities (Leard et al. 2020; Ghosh et al. 2020, 13, 2602).

Now, a new type of rail transit system can become a solution to urban traffic congestion and urban environmental pollution problems. The transportation system adopts a bridge-laying track design. While dispersing passenger flow for ground transportation, it does not occupy ground area. At the same time, the transportation system adopts electric drive, which can reduce air pollution and greenhouse gas emissions. The concept diagram of this electric drive transportation system is shown in Figure 1.1.

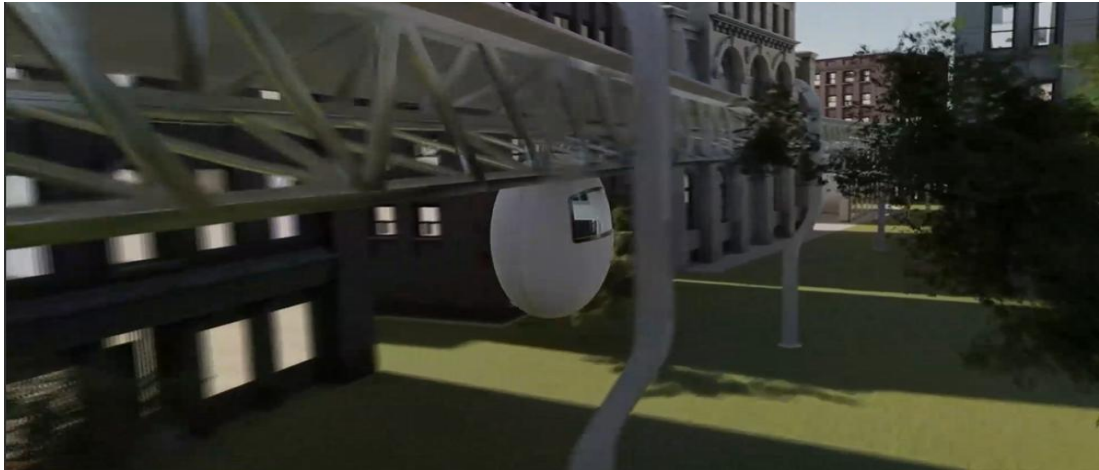


Figure 1.1. Transportation system concept map

1.2 Research status of battery technology at home and abroad

In the domestic research on rail system batteries, Zhang Zhiwen et al. (2025, 48(02):13-18) conducted a full-process optimization design of a hydrogen fuel cell system based on a multi-physics field coupling model for the innovative application of hydrogen fuel cell hybrid systems in rail transit equipment, taking a certain type of shunting locomotive as the research object. The system adopts an integrated architecture of "fuel cell stack + DC/DC converter + energy storage device", in which the anode hydrogen supply subsystem breaks through the traditional single circulation mode and innovatively proposes a composite hydrogen supply scheme of ejector and variable frequency circulation pump in parallel. Li Huiguang et al. (2023, 61(06):48-53) studied the power application of lithium titanate batteries in rail-type rubber-wheeled trains based on the special needs of rail transit equipment. Through a multi-stage iterative optimization method, it was determined that the battery module adopts a 3P91S series-parallel architecture and matches a dedicated BMS to achieve active balancing control. The key design parameters were verified by simulation, showing that within the rated voltage platform range of $480V \pm 5\%$, the system supports the continuous working condition requirement of the maximum charge and discharge rate of 3C, and the SOC working window is optimized to 30%-85%, effectively avoiding the risk of lithium plating of lithium titanate batteries. Hu Jingxian et al. (2015, 18(01):35-38) proposed a regenerative braking energy recovery and utilization system based on lithium-ion batteries to address the technical bottlenecks of the traditional resistance braking method used in urban rail transit vehicles, such as the increase in tunnel ambient temperature, the increase in vehicle weight,

and the waste of braking energy. The system adopts a modular energy storage unit topology structure, integrating a bidirectional DC/DC power converter and an intelligent energy management algorithm.

In foreign research on rail system batteries, Tian Q et al. (2018, 366) extracted the operating conditions of the train auxiliary battery system by collecting information on lithium titanate battery packs and single cells in the auxiliary battery system of rail vehicles in real time, and focused on establishing a battery floating charge test under the influence of factors such as temperature and voltage. Then, the battery aging status information was analyzed. Combining the thermodynamic and kinetic characteristics of the power battery, the law of change of the characteristic parameters of the power battery with the floating charge amount of the battery was established, and the degradation mechanism of the power battery was determined. Amin M M et al. (2021, 45(13): 18827-18845) proposed a BESTrain system based on mobile battery energy storage to address the grid congestion problem caused by the uncertainty of renewable energy. A multi-objective mixed integer linear programming model was constructed, and a two-stage stochastic technology was combined to deal with wind power and demand fluctuations, and to optimize the train charging and discharging strategy and power plant scheduling. Manusov Z V et al. (2018, 177(1):012024-012024) pointed out that the voltage imbalance problem of the power supply system caused by the 2×25 kV AC system used in urban rail transit was caused by the access mode of traction substation. By comparing the negative sequence components generated by three-phase transformers and Scott transformers, a negative sequence voltage evaluation model based on phase coordinate and symmetrical component method was proposed.

1.3 Dual-battery System Overview

In transportation vehicles, the high-rate lithium battery of the dual-battery system is used in high-power demand scenarios (such as acceleration and uphill), providing instantaneous high current output. The low-rate lithium battery powers auxiliary systems (such as on-board electronic equipment) and low-power loads, optimizing the efficiency of low-power scenarios. (Benmouiza et al. 2018, 43, 3512-3519) If the dual-battery system is combined with a fuel cell as a medium-power supplement, each energy unit operates within the optimal power range, the overall efficiency can be improved by 31.4%, and the battery life can be

extended by reducing the depth of discharge (DOD) of a single battery. Through the power allocation strategy, the system weight and volume are also reduced, and the driving range is increased. (Carlos et al. 2024, 16, 2110) The addition of supercapacitors to the dual-battery system can not only reduce energy loss, but also improve the acceleration performance of the vehicle. (Selvakumar et al. 2024, 115, 109099) The use of supercapacitors and batteries with high-precision power and specific energy is the most popular hybrid combination (Castaings et al. 2016, 163, 190-200). The dual-battery system composed of a photovoltaic cell and a brake energy storage system on the vehicle needs to deal with complex control situations. The application of artificial intelligence control methods can make the vehicle run more smoothly and have stronger acceleration capabilities. (Ron Carter, S.B et al. Journal info missing). There are also dual-battery systems that combine electric vehicle hybrid energy storage systems (HESS) with wireless power transfer and regenerative braking functions. (Pasupuleti et al. 2023, 59, 3785-3794; Fonseca de Freitas et al. 2023, 16, 7620)

1.4 The analysis to the advantages and disadvantages to the dual-battery system

1.4.1 The advantages of the dual-battery system

The dual-battery system offers a number of significant advantages that make it uniquely advantageous in the field of vehicle power and electrical equipment supply. First, a clear division of functions is one of the core advantages of the dual-battery system. The drive battery focuses on powering the vehicle's main motor drive unit, while the auxiliary battery is dedicated to providing a stable 24V voltage for cabin control systems (such as computers, sensors, displays, etc.) and electrical devices (such as USB or Type-C charging ports, air conditioning, entertainment equipment, etc.). The division of labor design avoids the efficiency loss of a single battery system when meeting both high-power electrical requirements and low-power electrical requirements, thereby significantly improving the operating efficiency of the overall system. Second, the dual battery system improves the reliability of the system. Because the two batteries operate independently, even if one of the batteries fails, the other battery will continue to work, ensuring the proper functioning of the vehicle's critical functions. Thirdly, the dual-battery system reduces the frequency and depth of charging and discharging of a single battery by distributing the load reasonably, thereby

extending the service life of the battery and reducing maintenance costs. Fourth, the dual-battery system can further improve energy efficiency by optimizing energy distribution through intelligent energy management strategies, such as recovering energy while the vehicle is braking and charging the auxiliary battery. These benefits make the dual battery system invaluable in improving vehicle performance, reliability, and passenger experience.

1.4.2 The disadvantages of the dual-battery system

Despite the many advantages of the dual-battery system, it also has some significant drawbacks. First, the complexity of the system has increased significantly. Dual-battery systems require additional control circuitry, energy management modules, and coordination mechanisms between cells, which not only makes design and manufacturing more difficult, but also increases the maintenance cost of the system. Second, the initial cost of a dual-battery system is higher. The manufacturing cost is much higher than that of a single-battery system due to the need to configure two batteries and the associated control equipment, and the maintenance and replacement costs of both batteries are also higher, which can put financial pressure on applications with limited budgets. Third, the dual battery system requires more installation space, which poses a challenge to the overall design layout of the vehicle, especially in models with limited space, which may affect the arrangement of other components or the optimization of the vehicle structure. Fourth, the configuration of a dual battery system will increase the overall weight of the vehicle, especially if a large capacity battery is required, and the increase in weight may have a negative impact on the energy consumption and dynamic performance of the vehicle. These shortcomings make the dual-battery system face certain challenges in promotion and application.

1.5 Research targets

The target of this thesis is to clarify the structural characteristics of the tram battery system of the transportation system, find the most suitable structure and dimensioning for its operation, make the system performance better and more reliable, and provide theoretical and technical support for the design and manufacture of new rail vehicles.

The component parameters of the dual-battery system are calculated, and the appropriate components of the dual-battery system are selected according to the component parameters, and the working state of the dual-battery system in different working environments is analyzed.

2 Method

2.1 Basic framework design of dual battery system

The dual batteries designed in this paper consist of a drive battery and an auxiliary battery. The drive battery is primarily responsible for powering the vehicle's main motor drive unit via the charging unit and charging the auxiliary battery through the voltage conversion circuit at the same time. The auxiliary battery mainly provides a stable 24V voltage for the cabin control system (including computers, sensors, displays, etc.) and various electrical equipment (such as USB or Type-C charging ports, air conditioners, entertainment equipment, etc.) to ensure that these devices can continue to operate and avoid affecting the normal maintenance of the control system and the passenger's experience due to power interruption.

The voltage conversion circuit is responsible for reducing the voltage of the driving battery to the working voltage of the auxiliary battery (24V), thereby realizing the power supply of the driving battery to the auxiliary battery.

The configuration of a dual-battery tram is shown in Figure 2.1.

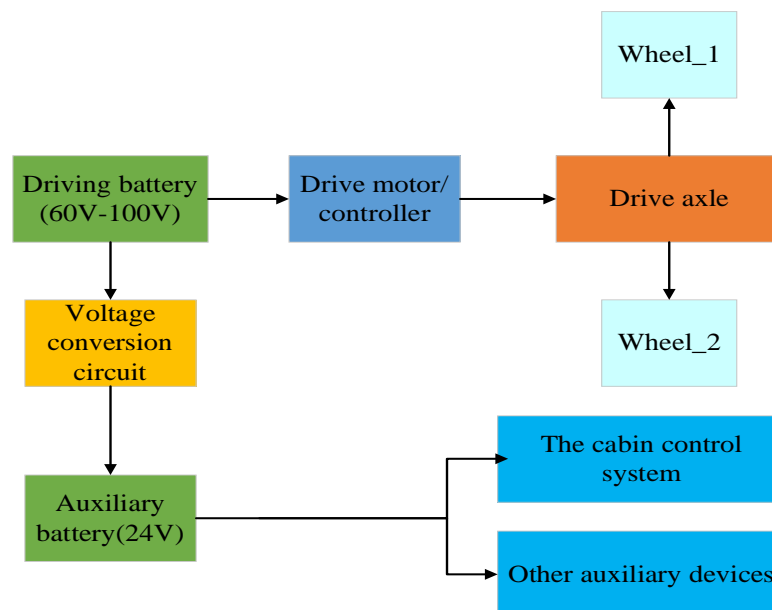


Figure 2.1. Tram configuration diagram with dual battery system

Battery detection units are added to the driving battery and the auxiliary battery respectively to detect the status of the driving battery and the auxiliary battery.

2.2 Auxiliary battery

2.2.1 Auxiliary battery design

The auxiliary battery shall provide continuous and stable power to the cockpit control system (computer, sensor, display, door operation) and other electrical equipment (USB-chargers, audio devices, lighting, air conditioning / heating / cooling) for the convenience of passengers, as shown in Figure 2.2.

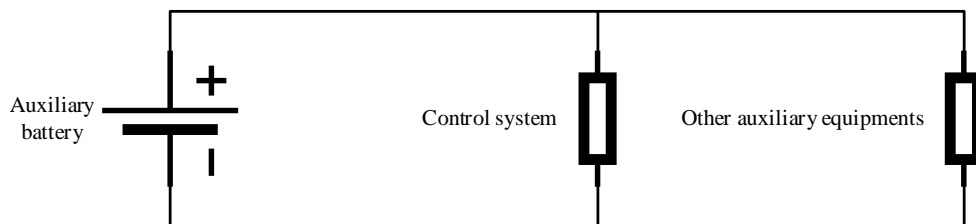


Figure2.2. Auxiliary battery general circuit diagram

2.2.2 Calculation of auxiliary battery related parameters and selection of components

The specific parameter requirements for auxiliary batteries are shown in Table 2.1.

Table 2.1. Auxiliary battery parameter requirements

| Parameters | The numeric value of the parameters |
|---|-------------------------------------|
| The required voltage of the auxiliary battery U_{ab} [V] | 24 |
| The required discharge time of the auxiliary battery T_{ab} [h] | 2 |

In each single cockpit, the power consumption of each auxiliary device is shown in Table 2.2.

Table 2.2. The power consumption of each auxiliary device

| Parameters | The numeric value of the parameters |
|---|-------------------------------------|
| The power consumption of lighting P_1 [W] | 15 |
| The power consumption of air conditioning / heating / cooling P_2 [W] | 160 |
| The power consumption of computer P_3 [W] | 45 |
| The power consumption of display P_4 [W] | 35 |
| The power consumption of sensors P_5 [W] | 55 |
| The power consumption of door operation P_6 [W] | 100 |
| The power consumption of communication system P_7 [W] | 25 |
| The power consumption of USB -chargers P_8 [W] | 25 |
| The power consumption of audio devices P_9 [W] | 20 |

The total power consumption (P_{sum}) of the auxiliary equipment in a single cockpit. The total power consumption of a single capsule auxiliary device (P_{sum}) is equal to the sum of the power consumption of each auxiliary device in a single capsule.

$$P_{\text{sum}} = \sum_{k=1}^9 P_k \quad (2.1)$$

According to Table n, the total power consumption (P_{sum}) of the auxiliary equipment in a single cockpit can be obtained, and the load current (I_{ab}) is calculated as follows:

$$I_{\text{ab}} = \frac{P_{\text{sum}}}{U_{\text{ab}}} \quad (2.2)$$

The capacity of the auxiliary battery (C_{ab}) is calculated as follows:

$$C_{\text{ab}} = I_{\text{ab}} \times T_{\text{ab}} \quad (2.3)$$

According to the parameter requirements of the obtained auxiliary battery, find a battery that meets the required auxiliary battery parameter requirements on the market and use it as the auxiliary battery.

2.3 Drive battery

2.3.1 Drive battery design

In each single capsule, the drive battery is responsible for powering the drive unit in the cockpit and charging the auxiliary battery, according to its function, the circuit diagram of the driving battery part is shown in Figure 2.3.

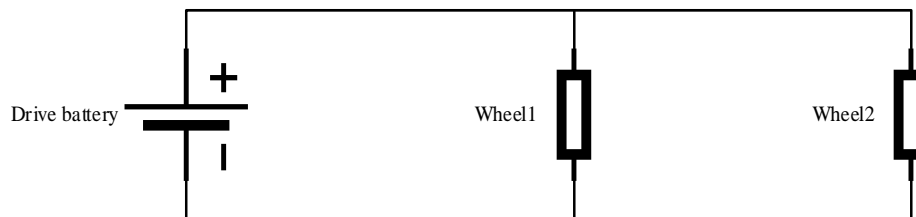


Figure 2.3. Drive battery general circuit diagram

2.3.2 The calculation of drive battery related parameters and components selection to the drive battery

When designing a drive battery, in addition to calculating the battery capacity based on the power requirements of the drive unit, factors such as auxiliary battery charging, reserve power, efficiency loss, and battery aging need to be considered. Therefore, additional capacity (C_{extra}) should be added to the drive battery to meet the additional needs during the charging process, ensure the reliability and stability of the system, and avoid failures caused by insufficient power or aging of the battery.

The specific parameter requirements of the drive battery are shown in Table 2.3.

Table 2.3. Drive battery parameter requirements

| Parameters | The numeric value of the parameters |
|------------|-------------------------------------|
|------------|-------------------------------------|

| | |
|--|------|
| Single cockpit drive unit load P_{il} [KW] | 5.5 |
| The discharge time of the drive battery T_{db} [h] | 0.75 |
| Maximum output voltage requirements for the drive battery $U_{db_o_max}$ [V] | 100 |
| Minimum output voltage requirements for drive batteries $U_{db_o_min}$ [V] | 60 |
| Additional battery capacity C_{extra} [Ah] | 52 |

In this thesis, a lithium iron phosphate battery (LiFePO₄) is used to construct the drive battery. Lithium iron phosphate batteries usually have a long service life, and the application of this type of battery can make the dual-battery system operate stably and reliably for a long time. In addition, compared to other lithium batteries, lithium iron phosphate batteries are more environmentally friendly and have less impact on the environment. (Huang et al. 2019, 22587-22597)

The output voltage of lithium iron phosphate as a function of battery charge is shown in Figure 2.4.

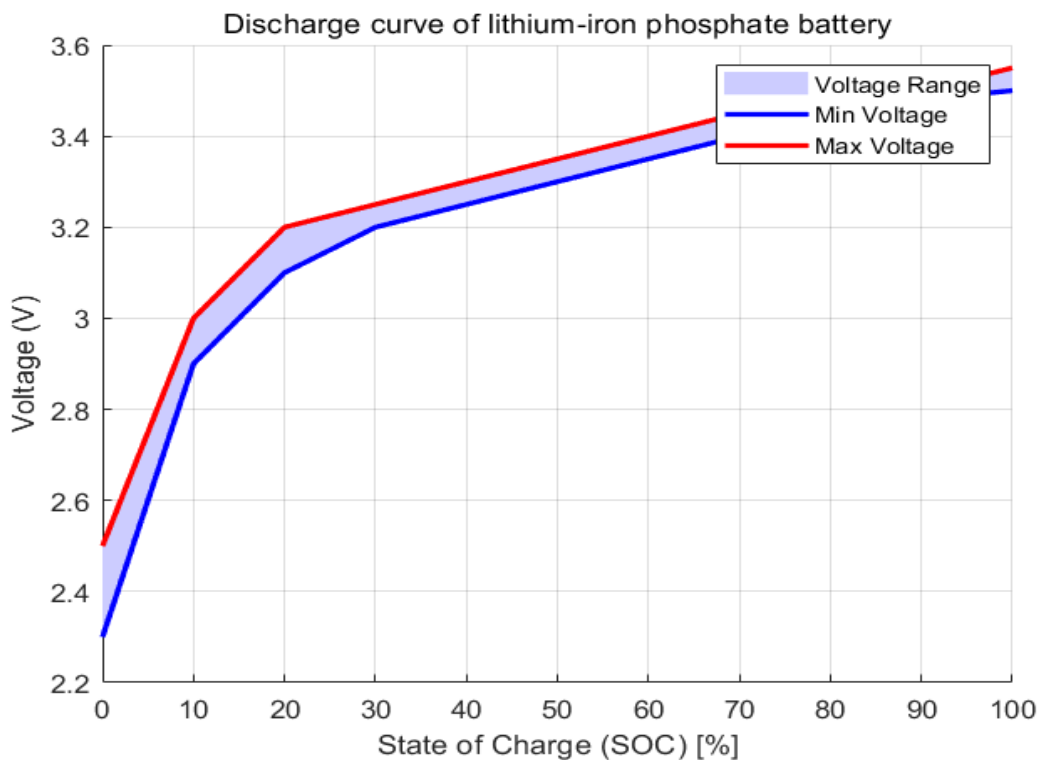


Figure 2.4. Discharge curve of lithium-iron phosphate battery (Li et al. 2022, 324-330)

According to the actual discharge curve of the lithium-iron phosphate battery, the output voltage of the drive battery is between 2.3~3.5V.

In order to more accurately reflect the working state of the battery in practical application, this thesis uses the output voltage range of the drive battery in actual operation to determine the maximum output voltage and minimum output voltage of the lithium-iron phosphate battery, so as to calculate the relevant parameters with the design, so the parameters of a single lithium-iron phosphate battery used in this paper are shown in Table 2.4.

Table 2.4. Parameters of lithium-iron phosphate batteries used

| Parameters | The numeric value of the parameters |
|--------------------------------------|-------------------------------------|
| Nominal voltage U_n [V] | 3.2 |
| Maximum output voltage U_{max} [V] | 3.5 |
| Minimum output voltage U_{min} [V] | 2.3 |
| Monomer length L_s [mm] | 101 |
| Monomer width W_s [mm] | 32 |
| Unit height H_s [mm] | 192 |
| Rated operating current I_n [A] | 120 |
| Rated charging current I_{ni} [A] | 20 |

In this thesis, several single lithium-iron phosphate batteries will be connected in series to meet the specific parameter requirements of the drive battery. By connecting multiple battery cells in series to form a battery pack, not only can the overall performance of the system be improved, but also a more balanced battery load distribution can be achieved, which in turn will improve the life of the battery. In addition, the series array can effectively increase the output voltage of the system to meet the voltage requirements of the load.

Based on the parameter requirements of the drive battery, the following calculations are carried out to design a lithium-iron phosphate battery drive system that meets these requirements.

The number of strings (N) of the drive battery pack should meet the following two conditions:

$$N \times U_{max} \leq U_{db_o_max} \quad (2.4)$$

$$N \times U_{min} \geq U_{db_o_min} \quad (2.5)$$

In order to ensure the performance of the battery pack, reduce the overall cost of the system as much as possible, and improve the economic benefits, the minimum number of battery strings that meet the requirements of the driving battery parameters is used in this paper.

Therefore, the voltage of the drive battery during cockpit operation (U_{db}) is calculated as:

$$U_{db} = N \times U_n \quad (2.6)$$

The output voltage of the drive battery when the drive battery is fully charged:

$$U_{db_max} = N \times U_{max} \quad (2.7)$$

The output voltage of the drive battery when the SOC of the drive battery is low:

$$U_{ab_min} = N \times U_{min} \quad (2.8)$$

The load current (I_{load}) is calculated as:

$$I_{load} = \frac{P_{tl}}{U_{db}} \quad (2.9)$$

When calculating the capacity of the drive battery (C_s), the additional capacity (C_{extra}) added to the drive battery is added.

$$C_s = I_{load} \times T_{db} + C_{extra} \quad (2.10)$$

Battery packs formed by a single lithium-iron phosphate battery connected in series will be housed in a battery box to protect and secure these battery modules.

2.4 Voltage conversion circuit

2.4.1 Voltage conversion circuit design

This article uses the topology Buck step-down circuit to obtain the voltage conversion circuit.

In this step-down circuit, a MOSFET is used as a switching device.

The basic structure diagram of the Buck step-down circuit applied in this paper is shown in Figure 2.5.

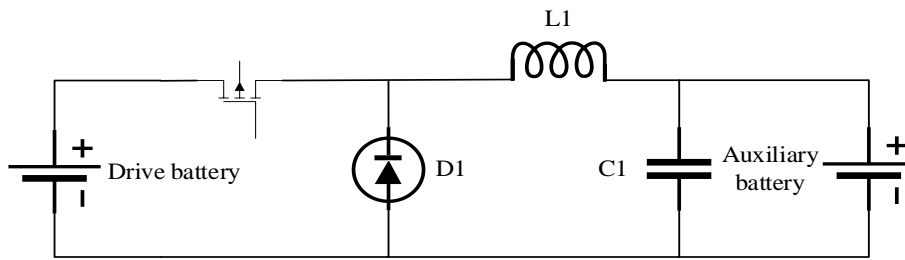


Figure 2.5. Basic structure diagram of Buck step-down circuit

A filter capacitor C2 is added to the conversion circuit to filter out high-frequency clutter generated by electromagnetic pulses. At the same time, diodes D2 and D3 are added to the conversion circuit, and the unidirectional conduction characteristics of the diodes are used to prevent reverse charging, so as to ensure that the drive battery can charge the auxiliary battery stably and continuously, and the topology of the buck step-down circuit is shown in Figure 2.6.

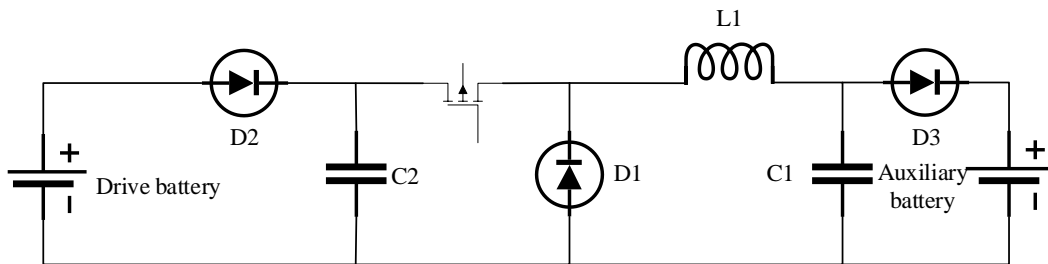


Figure 2.6. Buck step-down circuit topology

A feedback network composed of control elements is used to adjust the duty cycle of the MOSFET in real time according to the actual output voltage of the conversion circuit, so that the output voltage of the conversion circuit is always 24V.

The feedback network model is shown in Figure 2.7.

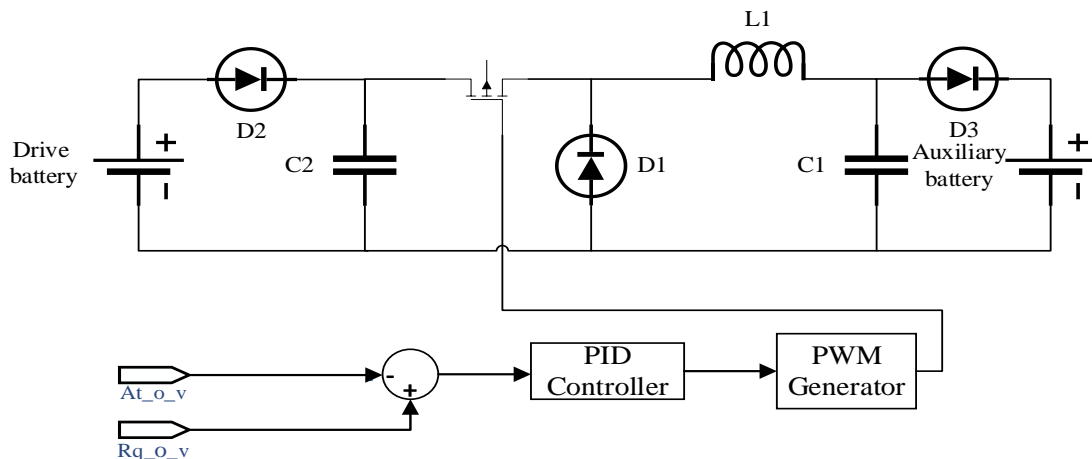


Figure 2.7. Feedback network circuit diagram

The SUM module calculates the difference between the required output voltage of the Buck step-down circuit (Rq_o_v) and the actual output voltage of the Buck step-down circuit (At_o_v) measured by the voltage detection device. The PID controller outputs a control signal based on this difference. The PWM generator adjusts the duty cycle of the MOSFET based on this control signal, so that the Buck circuit can continuously and stably output a 24V voltage.

2.4.2 Parameter calculation and selection of conversion circuit components

Considering that the voltage of the auxiliary battery may exceed 24V when its power is high, in order to ensure that the drive battery can still charge the auxiliary battery, the output voltage of the conversion circuit should be slightly higher than 24V, so the parameter requirements of the Buck step-down circuit are shown in Table 2.5.

Table 2.5. The parameter requirements of the Buck step-down circuit

| Parameters | The numeric value of the parameters |
|--|-------------------------------------|
| Buck step-down circuit output current I_{bo} [A] | 5 |
| Chip switching frequency f_{sw} [KHz] | 100 |
| Buck step-down circuit output voltage U_{bo} [V] | 27 |

The input voltage of the conversion circuit is the drive battery voltage (U_{db}), and its maximum input voltage and minimum input voltage are the output voltage (U_{db_max}) when the driving battery is fully charged and the output voltage (U_{db_min}) when the SOC of the drive battery is extremely low, respectively.

Since the output voltage of the driving battery changes during the discharge process, when the driving battery is in a fully charged state or close to a fully charged state, the input voltage of the conversion circuit reaches a maximum value (U_{bi_max}) which is the maximum output voltage (U_{db_max}) of the driving battery. After that, as the driving battery power decreases, the input voltage of the conversion circuit also continues to decrease. When the driving battery power is close to 0, the input voltage of the conversion circuit reaches a minimum

value (U_{bi_min}) which is the minimum output voltage (U_{db_min}) of the driving battery. However, no matter how much the input voltage of the conversion circuit is, the output voltage of the conversion circuit should always be the auxiliary battery voltage (U_{ab}), so the duty cycle range of the Buck step-down circuit is:

$$\frac{U_{bo}}{U_{bi_max}} \leq D \leq \frac{U_{bo}}{U_{bi_min}} \quad (2.11)$$

The relationship between the ripple current (ΔI_1) and the Buck step-down circuit output current (I_{bo}) is as follows:

$$\Delta I_1 = 0.4 \times I_{bo} \quad (2.12)$$

The inductance required for this conversion circuit is:

$$L = \frac{(U_{bi} - U_{bo})}{f_{sw} \times \Delta I_1} \times D \quad (2.13)$$

When the input voltage of the buck circuit is at the minimum value (U_{bi_min}), the required inductance value is the minimum:

$$L = \frac{(U_{bi_min} - U_{bo})}{f_{sw} \times \Delta I_1} \times \frac{U_{bo}}{U_{bi_min}} \quad (2.14)$$

When the input voltage of the buck circuit is at its maximum value (U_{bi_max}), the required inductance value is the largest:

$$L = \frac{(U_{bi_max} - U_{bo})}{f_{sw} \times \Delta I_1} \times \frac{U_{bo}}{U_{bi_max}} \quad (2.15)$$

When the input voltage of the buck circuit is at the maximum value (U_{bi_max}), if the inductance value is too small, the current ripple amplitude will increase, which will cause the heat of the inductor to rise, and there is a risk of damaging the component. Therefore, in the design, the inductance value when the input voltage is at the maximum value should be used as the lower limit standard of the selected inductance value.

Considering that the larger the inductance value, the higher the corresponding device cost, in order to take into account both circuit safety and economy, this design selects the inductance value when the input voltage is the maximum value (U_{bi_max}) as the basis for the final selection of the inductor device.

The relationship between ripple voltage and output voltage is:

$$\Delta U_{\text{out}} = 0.01 \times U_{\text{bo}} \quad (2.16)$$

The capacitor is a voltage regulator element in the conversion circuit, and its calculation formula is:

$$C = \frac{\Delta I_1}{8 \times f_{\text{sw}} \times \Delta U_{\text{out}}} \quad (2.17)$$

When the switch is closed, the diode D1 should be in the off state. At this time, the current in the MOSFET is the same as the output current (I_{bo}) of the conversion circuit. When the switch is open, the current in the MOSFET is 0. The calculation formula for the effective value of the current in the MOSFET ($I_{\text{rms_mos}}$) is:

$$I_{\text{rms_mos}} = I_{\text{bo}} \times \sqrt{D} \quad (2.18)$$

The rated current ($I_{\text{n_mos}}$) of the selected MOSFET should be higher than its on-state current ($I_{\text{rms_mos}}$). However, the duty cycle of the Buck step-down circuit is constantly changing, the on-state current ($I_{\text{rms_mos}}$) of the MOSFET is also constantly changing, and its range is:

$$I_{\text{bo}} \times \sqrt{\frac{U_{\text{bo}}}{U_{\text{bi_max}}}} \leq I_{\text{rms_mos}} \leq I_{\text{bo}} \times \sqrt{\frac{U_{\text{bo}}}{U_{\text{bi_min}}}} \quad (2.19)$$

To improve safety, the rated current ($I_{\text{n_mos}}$) of the selected MOSFET should be higher than its maximum on-current.

The conduction current ($I_{\text{rms_dio}}$) of the diode, i.e. the average current, is:

$$I_{\text{rms_dio}} = I_{\text{bo}} \times \sqrt{1 - D} \quad (2.20)$$

Considering that the duty cycle of the conversion circuit is constantly changing, the conduction current range of the diode is:

$$I_{\text{bo}} \times \sqrt{1 - \frac{U_{\text{bo}}}{U_{\text{bi_min}}}} \leq I_{\text{rms_dio}} \leq I_{\text{bo}} \times \sqrt{1 - \frac{U_{\text{bo}}}{U_{\text{bi_max}}}} \quad (2.21)$$

To improve safety, the rated current ($I_{\text{n_dio}}$) of the selected MOSFET should be higher than its maximum on-current.

The rated voltage of MOSFET ($U_{\text{n_mos}}$) and the rated voltage of diode ($U_{\text{n_dio}}$) should be higher than the input voltage of conversion circuit (U_{bi}). In order to improve safety as much as possible, the rated voltage of MOSFET ($U_{\text{n_mos}}$) and the rated voltage of diode ($U_{\text{n_dio}}$) should be higher than the maximum value of the input voltage of conversion circuit ($U_{\text{bi_max}}$).

The switching frequency of the selected PWM Generator should reach the required chip switching frequency (f_{sw}).

2.5 Optimization to the dual-battery system

2.5.1 Auxiliary battery protection

The auxiliary battery is a lithium battery. When the lithium battery is fully charged, it will be under great electrochemical pressure. This electrochemical pressure will affect the chemical substances inside the battery. If the driving battery fully charges the auxiliary battery every time, it will cause the capacity of the auxiliary battery to decrease, reducing the service life of the auxiliary battery. In addition, the auxiliary battery cannot be completely discharged. If the power of the lithium battery is too low, the negative electrode material of the battery may undergo incomplete lithium iron insertion/deinsertion reaction. This incomplete chemical reaction will cause structural damage to the negative electrode material, reduce the energy storage capacity of the battery, and cause the battery capacity to decrease (Zhou et al. 2021, 53(1): 55-62). In order to extend the service life of the auxiliary battery, it is required that when the power of the auxiliary battery reaches 80%, the driving battery stops charging the auxiliary battery, and when the power of the auxiliary battery drops below 60%, the driving battery starts charging the auxiliary battery, in this way, can not only protects the auxiliary battery, but also ensures that when the drive battery is disconnected or fails, the auxiliary battery always has enough power to keep the cabin running for a period of time.

Add switch devices between the drive battery and the conversion circuit to achieve the function of protecting the auxiliary battery.

The structure diagram of the dual battery system with auxiliary battery protection measures is shown in Figure 2.8.

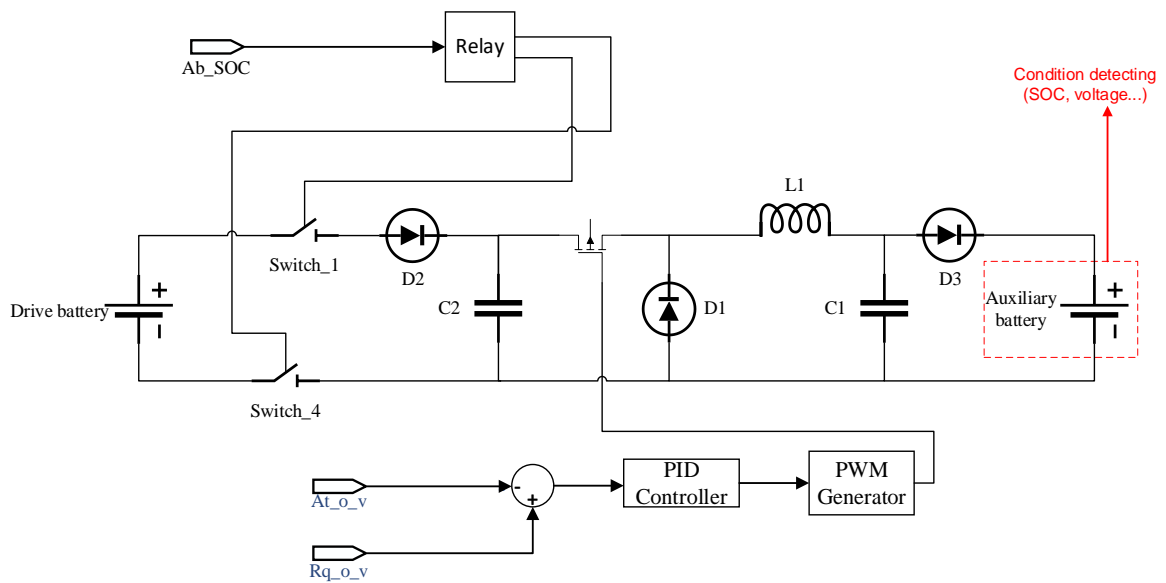


Figure 2.8. Dual battery system circuit diagram with auxiliary battery protection measures

In Simulink modeling, the control circuit with Relay module as the main component controls the opening and closing of Switch_1 and Switch_4. When the battery status detection device of the auxiliary battery detects that the power of the auxiliary battery (Ab_SOC) reaches 80%, the control circuit controls Switch_1 and Switch_4 to disconnect, and the drive battery stops charging the auxiliary battery. When the battery detection device detects that the power of the auxiliary battery (Ab_SOC) drops to 60%, the control circuit controls Switch_1 and Switch_4 to close, and the drive battery continues to charge the auxiliary battery.

2.5.2 Application of regenerative braking technology

This thesis applies regenerative braking technology to this transportation system. Compared with traditional mechanical braking, this technology converts the vehicle's kinetic energy into electrical energy by switching the electric motor on the electric vehicle from motor mode to generator mode when the electric vehicle decelerates or brakes, and stores this energy back into the battery, thereby improving energy efficiency, extending battery life, and improving overall energy efficiency (Li et al. 2024, 399(5): 73-77).

When the cabin is in a deceleration or braking state, the cabin's wheels are still rotating. At this time, the electric motor on the cabin switches from motor mode to generator mode to charge the drive battery. In this way, the kinetic energy of the two wheels when the cabin is decelerating or braking is converted into electrical energy, thereby increasing the cabin's

endurance. At the same time, an additional circuit is designed to prevent overcharging of the drive battery.

The circuit structure diagram of the driving battery part after applying the regenerative braking technology is shown in Figure 2.9.

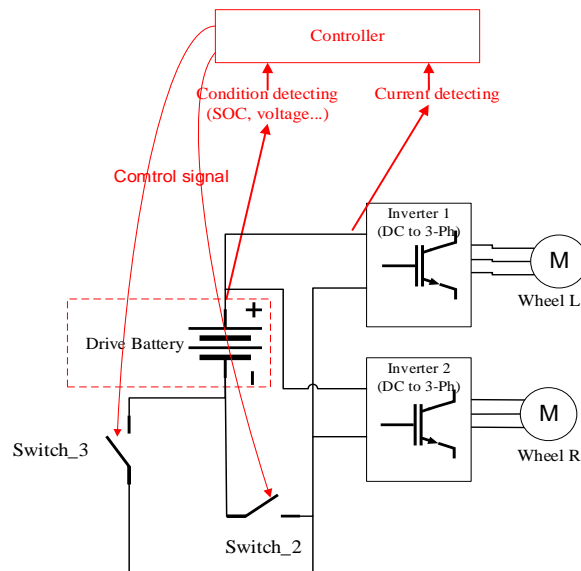


Figure 2.9. The circuit diagram of the drive battery circuit after applying regenerative braking technology

By adding a current detection device to measure the positive and negative current between the cabin load and the drive battery, it is known whether the current flows from the load to the drive battery or from the drive battery to the load.

The opening and closing of Switch_2 and Switch_3 are controlled by a control circuit composed of logic devices. The logic diagram of the control circuit is shown in Figure 2.10.

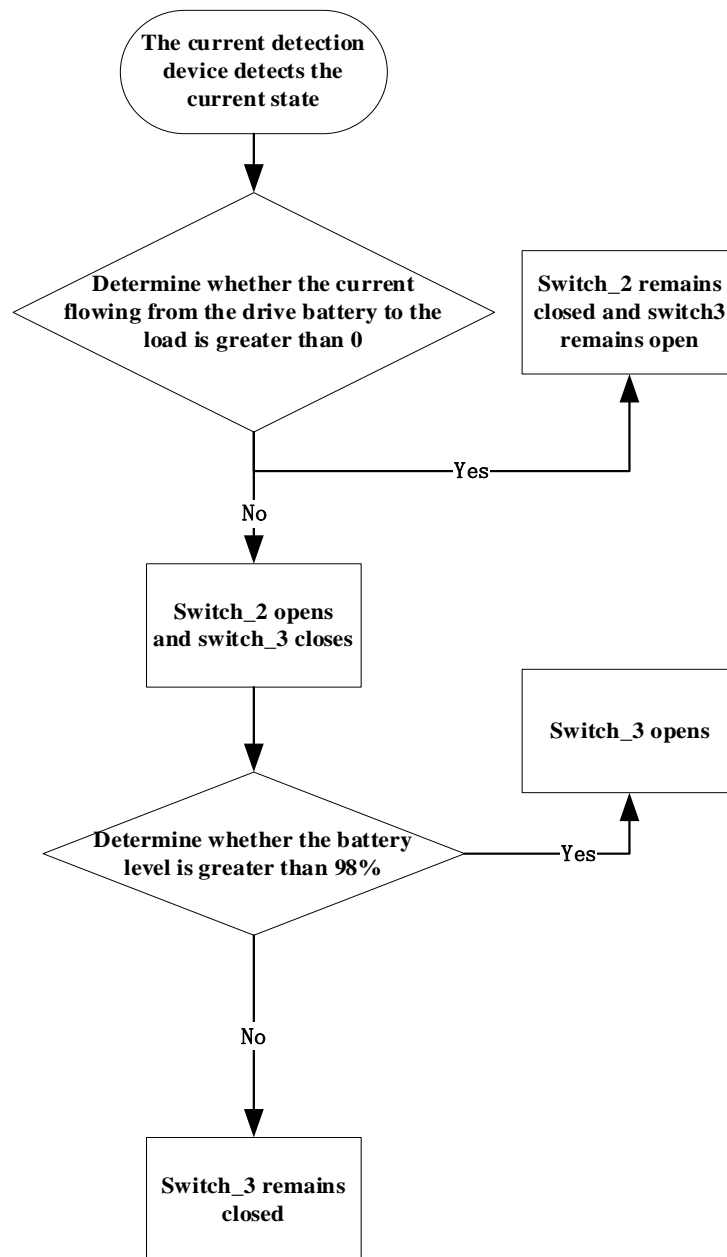


Figure 2.10. Flow chart of the opening and closing of the switch of the drive battery circuit

When the cabin is in a deceleration or braking state, the drive battery stops supplying power, and the cabin motor switches from motor mode to power generation mode to supply power to the drive battery. The current flows from the load to the drive battery, and the current detection device shows that the current is less than 0. Switch_2 is disconnected. Through the battery detection device, if the power of the drive battery is less than or equal to 98%, the control circuit controls Switch_3 to close and the drive battery enters the charging mode; if the battery power is greater than 98%, the control circuit controls Switch_3 to disconnect to prevent overcharging of the drive battery. When the cabin returns to normal operation from

braking or deceleration mode, the current flows from the drive battery to the load, and the current detection device shows that the current is greater than 0. The control circuit controls Switch_2 to close and Switch_3 to disconnect, and the drive battery supplies power to the load normally.

2.6 The calculation to the time that the capsule can be operational without the drive battery

When the driving battery runs out of power, the auxiliary battery will be responsible for powering the cockpit drive unit. At this time, the auxiliary battery not only provides voltage for the cockpit auxiliary equipment but also provides voltage for the cockpit drive power supply.

At this time, the output current (I_{oe}) of the auxiliary battery is:

$$I_{oe} = \frac{(P_{as} + P_{tl})}{U_{ab}} \quad (2.22)$$

In order to protect the auxiliary battery, the driving battery will stop charging the auxiliary battery when the auxiliary battery power reaches 80%, and when the auxiliary battery power is lower than 60%, the driving battery will start charging it, so the auxiliary battery power range is always maintained at 60%-80%, so the operating time (T_w) of the cockpit without auxiliary battery power supply is in the range of:

$$\frac{0.6 \times C_{ab}}{I_{oe}} \leq T_w \leq \frac{0.8 \times C_{ab}}{I_{oe}} \quad (2.23)$$

2.7 Environmental conditions to be considered

2.7.1 High temperature environment

In high temperature environments such as exposure to the sun and temperature rise in closed cabins, the chemical reaction rate inside the battery is significantly accelerated, which may increase the power output in the short term, but it also brings a series of potential risks. First, the accelerated reaction can easily lead to a further increase in battery temperature, causing

serious safety problems such as overheating, bloating, leakage, and even thermal runaway. Secondly, the battery capacity will decrease with the increase in temperature, and the internal resistance will increase, which will reduce the actual available energy of the battery. In addition, in order to maintain the safe operation of the system, the thermal management system (such as air conditioning, cooling fans, etc.) needs to work continuously, thereby increasing the energy consumption burden of the auxiliary system. Under high temperature conditions, the imbalance between battery cells is also more prominent, and the balancing system needs to intervene frequently, further increasing power consumption and system complexity. Long-term operation in an environment above 60°C will accelerate the performance degradation of lithium batteries, seriously shorten their service life, and significantly increase safety risks. (Wang et al. 2019, 43(9): 1464-1466,1491)

2.7.2 Low temperature environment

The performance of lithium batteries is also limited under low temperature conditions when the cabin stops working at night. The chemical reaction rate of the battery slows down, resulting in a decrease in its discharge capacity. Even if the battery is fully charged, it may not be able to release energy due to insufficient power, which appears as a "false charge". At the same time, low temperatures can cause the internal resistance of the battery to rise sharply and the output voltage to drop rapidly, which may be misjudged by the battery management system (BMS) as an undervoltage state and cut off the load, affecting the normal operation of the equipment. In order to improve the starting and operating capabilities under low temperatures, the system usually needs to preheat the battery through thermal management methods (such as PTC heaters), but this also brings additional energy consumption burdens. Overall, low temperatures will severely inhibit the output capacity and endurance performance of the battery, and limit the operating time of the equipment. (Wang et al. 2019, 43(9): 1464-1466,1491)

2.8 Drive battery replacement scheme

In the public transportation system of modern cities, the traditional charging method usually takes a long time, which seriously affects the operational efficiency of the vehicle. In order

to solve this problem, the automatic battery replacement system of the UDT passenger station came into being. The system enables fast and efficient battery replacement to ensure that the vehicle is back in operation in the shortest possible time. When the vehicle arrives at the battery swapping station, the system will automatically detect the battery level and health status of the vehicle's battery, and if the battery level is low or the battery status does not meet the requirements, the system will start the battery replacement process. With a highly automated robotic arm, the old battery is removed and replaced with a fully charged, healthy battery, ensuring that the vehicle can continue to be used for transportation.

After the vehicle enters the replacement station, the system uses positioning technology to accurately determine the vehicle's position and perform battery status detection. If the battery is eligible for replacement, the automated system quickly removes the old battery through a robotic arm and selects a fully charged and healthy battery from the battery storage area to automatically complete the installation. The entire process takes only less than one minute, which greatly reduces vehicle downtime and improves operational efficiency. Through this efficient battery swapping mode, the vehicle can be quickly restored to service without the need for a long period of charging, meeting the needs of high-frequency departures.

2.9 Decentralization of BMS systems – analysis

Battery Management System (BMS) is a key component in battery pack applications. It is responsible for monitoring and managing the status of the battery to ensure its safe and efficient operation. With the continuous development of electric drive technology, the technology of power battery systems is also constantly improving. As the brain of the power battery system, the battery management system (BMS) is also constantly upgrading and developing towards a decentralized architecture. (Luo et al. 2022, (4): 52-58)

Decentralization of BMS systems refers to the decentralization of the traditional centralized BMS architecture, managing and monitoring the battery pack in a distributed manner, which responds to the development trend of BMS.

This thesis adopts two independent battery detection systems to monitor the status of the drive battery and auxiliary battery, reflecting the decentralized characteristics of the BMS system, and sets up separate control circuits for the voltage conversion circuit and the drive

battery part to achieve the purpose of battery system optimization. The advantage of this design is that it improves the reliability and redundancy of the system, because a battery system failure will not affect the management of another battery. At the same time, it also enhances the flexibility and real-time performance of the system, and can independently optimize the charging and discharging process of each battery unit.

This decentralized structure also brings some challenges, including the need to effectively coordinate the information flow and communication of each detection system to ensure the coordination and efficient operation of the system. In addition, in order to improve the overall reliability of the system, redundant design and fault recovery mechanism must also be considered.

3 Result

3.1 Auxiliary battery parameters and models

Auxiliary battery parameter requirements are shown in Table 3.1.

Table 3.1. Auxiliary battery parameters

| Parameters | The numeric value of the parameters |
|--|-------------------------------------|
| Nominal voltage U_{ab} [V] | 24 |
| Rated capacity C_{ab} [Ah] | 40 |
| Battery response time t_{ab} [s] | 0.1 |
| Auxiliary battery total load P_{sum} [W] | 480 |

The battery model found in the market that meets the parameter requirements of the auxiliary battery is KH-LFP24600, its battery type is lithium battery, the material is Lifepo4, and its related parameters are shown in Table 3.2.

Table 3.2. The parameters of the battery used to be the auxiliary battery

| Parameters | The numeric value of the parameters |
|------------------------------|-------------------------------------|
| Voltage [V] | 24 |
| Rated voltage [V] | 27.6 |
| Weight [kg] | 20 |
| Maximum charging current [A] | 60 |

Its voltage meets the required auxiliary battery voltage (U_{ab}), its rated voltage is higher than the output voltage (U_{bo}) of the conversion circuit, and its maximum charging current is also higher than the output current (I_{bo}) of the conversion circuit. This type of battery can perform its work tasks stably and safely as an auxiliary battery without overheating.

3.2 The time that the capsule can be operational without the drive battery

Without the drive battery, the capsule can run for a period of time as shown in Table 3.3.

Table 3.3. The time that the capsule can be operational without the drive battery

| Parameters | The numeric value of the parameters |
|--|-------------------------------------|
| Minimum elapsed time $T_{w_min}[\text{min}]$ | 6 |
| Maximum operating time $T_{w_max}[\text{min}]$ | 7.8 |

3.3 Drive battery parameters

The drive battery parameters are shown in Table 3.4.

Table 3.4. Drive battery parameters

| Parameters | The numeric value of the parameters |
|--|-------------------------------------|
| The number of strings of single lithium iron phosphate batteries used N | 27 |
| Nominal voltage $U_{db}[\text{V}]$ | 86.4 |
| Maximum output voltage of driving battery $U_{db_max}[\text{V}]$ | 94.5 |
| Driving battery minimum output voltage $U_{db_min}[\text{V}]$ | 62.1 |
| Rated capacity $C_{db}[\text{Ah}]$ | 100 |

3.4 Parameters and models of conversion circuit related components

The parameters of each component of the Buck step-down circuit are shown in Table 3.5.

Table 3.5. The parameters of each component of the Buck step-down circuit

| Parameters | The numeric value of the parameters |
|--|-------------------------------------|
| Inductor Component Inductance $L[\mu\text{H}]$ | 97 |
| Capacitor element capacitance value $C[\mu\text{F}]$ | 10 |

| | |
|---|------|
| MOSFET on-current $I_{rms_mos}[A]$ | 3.3 |
| The minimum voltage that the MOSFET needs to withstand $U_{bi_max}[V]$ | 94.5 |
| The conduction current of the diode $I_{rms_dio}[A]$ | 3.76 |
| The minimum voltage that the diode needs to withstand $U_{bi_max} [V]$ | 94.5 |
| The chip switching frequency of the selected PWM Generator $f_{sw}[KHz]$ | 100 |

An inductor element with an inductance value of L is selected as the inductor element in the conversion circuit, and a capacitor element with a capacitance value of C is selected as the capacitor element in the conversion circuit.

The selected MOSFET model is IRFH5015PbF, which is an N-channel Power MOSFET. Its specific parameters are shown in Table 3.6.

Table 3.6. The parameters of IRFH5015PbF MOSFET

| Parameters | The numeric value of the parameters |
|-------------------|-------------------------------------|
| Withstand voltage | 150V |
| Rated current | 13A |

This type of MOSFET can withstand the maximum input voltage of the conversion circuit, and its rated current also meets the requirements for the MOSFET rated current in the conversion circuit.

The diode model selected is UF4007, and its specific parameters are shown in Table 3.7.

Table 3.7. The parameters of UF4007 diode

| Parameters | The numeric value of the parameters |
|-------------------|-------------------------------------|
| Withstand voltage | 1000V |
| Rated current | 30A |

This type of diode can withstand the maximum input voltage of the conversion circuit, and its rated current also meets the requirements for the rated current of the diode in the conversion circuit.

The selected PWM Generator model is the DC-DC dedicated PWM controller chip LM5116 (TI company), and its specific parameters are shown in Table 3.8.

Table 3.8. The parameters of LM5116 (TI company) PWM Generator

| Parameters | The numeric value of the parameters |
|--------------------------|-------------------------------------|
| Output voltage range | 11.215V~80V |
| Chip switching frequency | 50KHz-1MHz |

The switching frequency of this model PWM Generator reaches the required chip switching frequency (f_{sw}).

3.5 Dual-battery system modeling and simulation

In Simulink modeling, Scopes are used as a battery detection unit to detect the status of the drive battery and auxiliary battery.

A complete circuit model of the dual-battery system is shown in Figure 3.1.

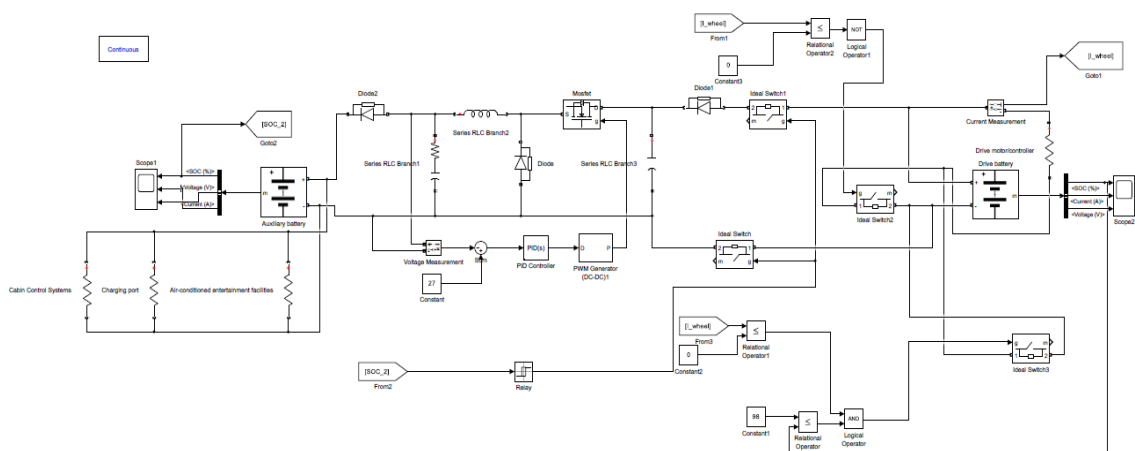


Figure 3.1. Complete circuit model of the dual-battery system

The changes of auxiliary battery voltage and driving battery voltage over time are shown in Figure 3.2 and Figure 3.3 respectively.

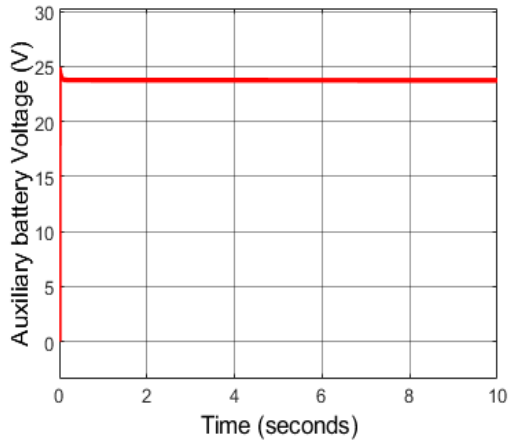


Figure 3.2. Auxiliary battery voltage

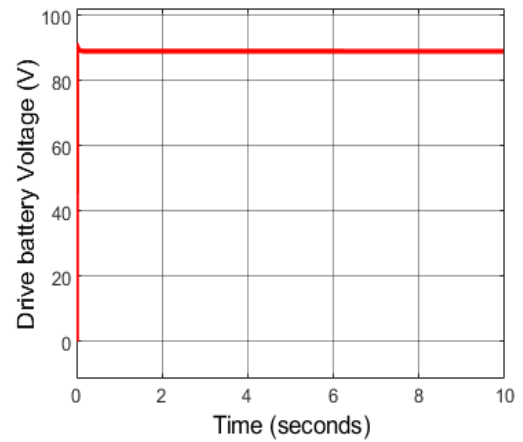


Figure 3.3. Drive battery voltage

From Figure 3.2 and Figure 3.3, we can see that the voltage of the auxiliary battery is always maintained at around 24V and the voltage of the drive battery is always maintained at around 86.4V.

The images of the driving battery SOC changing over time and the auxiliary battery SOC changing over time are shown in Figures 3.4 and 3.5 respectively.

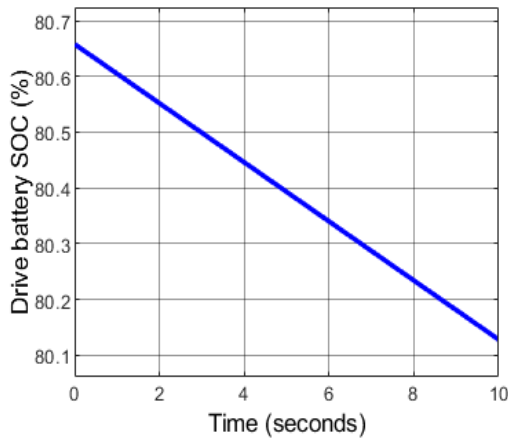


Figure 3.4. Drive battery SOC

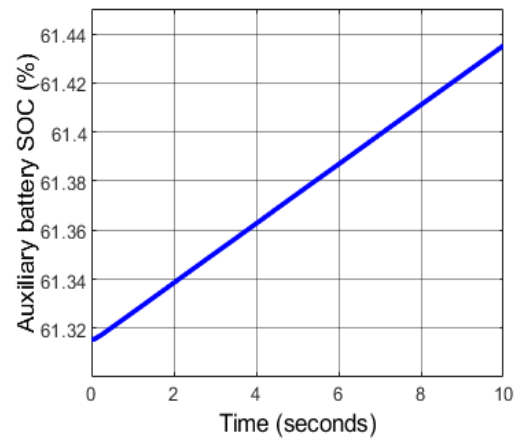


Figure 3.5. Auxiliary battery SOC

It can be seen from Figures 3.4 and 3.5 that as the SOC of the drive battery decreases, the SOC of the auxiliary battery increases, and the drive battery successfully charges the auxiliary battery.

Adjust the initial charge of the auxiliary battery module to nearly 80% to verify whether the II output voltage (U_{bo}) of the voltage conversion circuit is sufficient to continue charging the auxiliary battery when the auxiliary battery SOC is high.

When the auxiliary battery is charged, its SOC curve is shown in Figure 3.6.

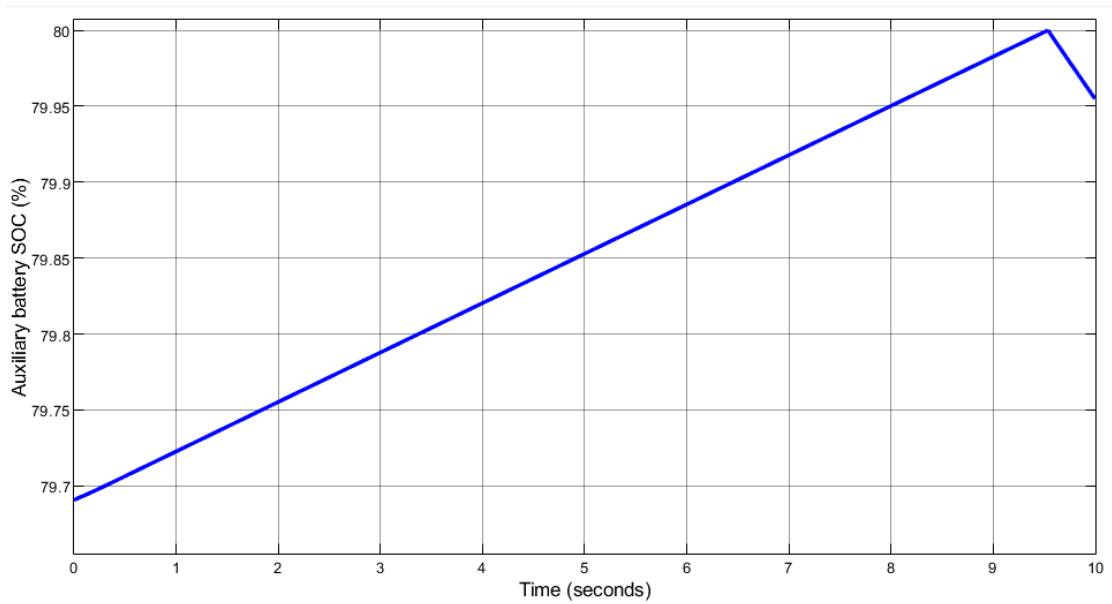


Figure 3.6. Auxiliary battery charging curve

When the auxiliary battery is discharged, its SOC curve is shown in Figure 3.7.

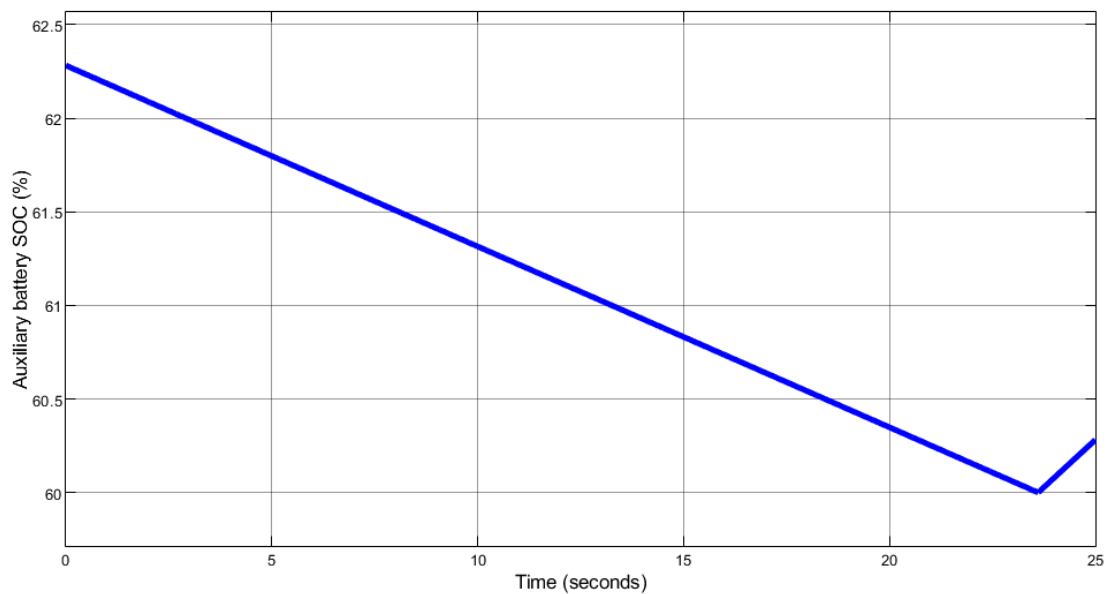


Figure 3.7. Auxiliary battery discharge curve

As can be seen from Figure 3.6 and Figure 3.7, when the auxiliary battery SOC is high, the drive battery can still charge the auxiliary battery. When the auxiliary battery SOC reaches 80%, the drive battery stops charging the auxiliary battery to protect the auxiliary battery. When the auxiliary battery is discharged to 60%, the drive battery starts charging the auxiliary battery again to ensure that when the drive battery fails, the auxiliary battery still has enough power to power the cockpit drive unit.

4 Conclusions

This thesis focuses on the design and optimization of the dual-battery system. By analyzing the advantages and disadvantages of the system, a deeper understanding of the dual-battery system is provided. By considering a variety of conditions and emergencies that affect the working state of the dual-battery system, the fault tolerance of the dual-battery system can be maximized. By setting up independent battery detection systems and control circuits for the drive battery and auxiliary battery respectively, the decentralization of the battery management system (BMS) is achieved. Through the analysis and modeling of the dual-battery system, the role of the drive battery and auxiliary battery in the system and their collaborative working principles are deeply explored. The design of the dual-battery system can effectively solve the endurance and stability problems of the single-battery system, while ensuring the efficient operation of the vehicle, improving the redundancy and safety of the system.

Through a detailed analysis of the dual-battery system, the functional configuration of the drive battery and the auxiliary battery is clarified. The drive battery is mainly responsible for providing power to the vehicle's main motor drive unit through the charging device, and charging the auxiliary battery at the same time. The auxiliary battery mainly provides a stable 24V voltage for the cockpit control system (including computers, sensors, display screens, etc.) and various power-consuming devices (such as USB or Type-C charging ports, air conditioners, entertainment equipment, etc.) to ensure that these devices can continue to work. The dual-battery system is modeled based on the basic working principle of the dual-battery system, the battery's working mode and voltage conversion requirements, and the feasibility of the system design is further verified through Simulink simulation. The simulation results show that on the basis of reasonable configuration of voltage and power consumption requirements, the dual-battery system can provide stable power support efficiently and safely.

As part of the design of a new urban rail transit system, this solution accelerates the research and development of a new transportation system that is beneficial to urban environmental protection, and has important social significance for the development of global environmental protection. However, although this paper provides a detailed design scheme

for the dual-battery system, how to ensure that the dual-battery system does not conflict or be inconsistent with other electronic and mechanical systems of the vehicle when working together is still a key issue that needs to be solved in future research.

References

- Namrata, and N D Wagh. “A Review on Atmospheric Dispersion System for Air Pollutants Integrated with GIS in Urban Environment.” *Nature environment and pollution technology* 21.4 (2022): 1553–1563. Web.
- Elmi, A, and N Al Rifai. “Pollutant Emissions from Passenger Cars in Traffic Congestion Situation in the State of Kuwait: Options and Challenges.” *Clean technologies and environmental policy* 14.4 (2012): 619–624. Web.
- Vallejo, Fidel et al. “Hybrid Porous Media Gasification of Urban Solid Waste Pre-Treated by Hydrothermal Carbonization.” *PloS one* 18.9 (2023): e0291838–e0291838. Web.
- Zhou, Bodong et al. “Large-Scale Traffic Congestion Prediction Based on Multimodal Fusion and Representation Mapping.” *2022 IEEE 9th International Conference on Data Science and Advanced Analytics (DSAA)*. IEEE, 2022. 1–9. Web.
- Huang, Zhiran, and Becky P. Y Loo. “Urban Traffic Congestion in Twelve Large Metropolitan Cities: A Thematic Analysis of Local News Contents, 2009-2018.” *International journal of sustainable transportation* 17.6 (2023): 592–614. Web.
- Zhang Zhiwen, Huang Yongcong, Xie Zhuangyou, et al. Architecture design and test verification of hydrogen fuel cell system for rail transit[J]. *Electric Locomotive & Urban Rail Vehicle*, 2025, 48(02): 13-18
- Li Huiguang, Shao Kecheng. Research on the application of lithium titanate batteries in rail transit vehicles[J]. *Rolling Stock Railway*, 2023, 61(06): 48-53
- Hu Jingxian, Song Wenji, Lin Shili, et al. Application of 1500V urban rail transit lithium battery energy storage system[J]. *Urban Rail Transit Research*, 2015, 18(01): 35-38
- Tian Q. Research on application of lithium titanate battery in auxiliary system of rail vehicle[J]. *IOP Conference Series: Materials Science and Engineering*, 2018, 366
- Amin M M , Mohammad H , Kazem Z , et al. Network-constrained rail transportation and power system scheduling with mobile battery energy storage under a multi-objective two-

- stage stochastic programming[J]. *International Journal of Energy Research*, 2021, 45(13): 18827-18845.
- Manusov Z V ,Bumtsend U ,Demin V Y .Analysis of the power quality impact in power supply system of Urban railway passenger transportation – the city of Ulaanbaatar[J].*IOP Conference Series: Earth and Environmental Science*,2018,177(1):012024-012024.
- Huang, Qianwen, Yun-Yang Lee, and Burcu Gurkan. “Pyrrolidinium Ionic Liquid Electrolyte with Bis(Trifluoromethylsulfonyl)Imide and Bis(Fluorosulfonyl)Imide Anions: Lithium Solvation and Mobility, and Performance in Lithium Metal–Lithium Iron Phosphate Batteries.” *Industrial & engineering chemistry research* 58.50 (2019): 22587–22597. Web.
- Li, Yuhong et al. “Research on Discharge Characteristics of Lithium Batteries in Low Temperature Environment.” *2022 3rd International Conference on Advanced Electrical and Energy Systems (AEES)*. IEEE, 2022. 324–330. Web.
- Zhou Yafu, Sun Xiaoxiao, Huang Lijian, et al Estimation of the state of health of lithium batteries for the whole life cycle[J]. *Journal of Harbin Institute of Technology*, 2021, 53(1): 55-62 (Li et al. 2024, 399(5): 73-77)
- Li Peiqing, Wu Xingkang, Chen Yikai, et al Research on regenerative braking composite control of tram for ECE regulations[J]. *Mechanical Design and Manufacturing*, 2024, 399(5): 73-77
- Wang Weiqiang, Zhang Li, Zhang Ji, et al Parameter Identification and Verification of LiFePO₄ Battery Model at High and Low Temperatures[J]. *Chinese Journal of Power Sources*,2019,43(9): 1464-1466,1491
- Luo Bin. Research on Improving the Communication Quality of Daisy Chain in BMS System of Power Battery for New Energy Vehicles[J]. *Xiamen Science and Technology*, 2022, (4): 52-58
- Leard, B.; McConnell, V. Progress and Potential for Electric Vehicles to Reduce Carbon Emissions; No. 20-24; Resources for the Future: Washington, DC, USA, 2020.
- Ghosh, A. Possibilities and challenges for the inclusion of the electric vehicle (EV) to reduce the carbon footprint in the transport sector: A review. *Energies* 2020, 13, 2602.

- Benmouiza, K.; Cheknane, A. Analysis of proton exchange membrane fuel cells voltage drops for different operating parameters. *Int. J. Hydrogen Energy* 2018, 43, 3512–3519.
- Carlos, A. Improving Sustainability in Urban and Road Transportation: Dual Battery Block and Fuel Cell Hybrid Power System for Electric Vehicles. *Sustainability* 2024, 16, 2110.
- Selvakumar, R.B.; Vivekanandan, C.; et al. Energy management of a dual battery energy storage system for electric vehicular application. *Comput. Electr. Eng.* 2024, 115, 109099.
- Castaings, A.; Lhomme, W.; Trigui, R.; Bouscayrol, A. Comparison of energy management strategies of a battery/supercapacitors system for electric vehicle under real-time constraints. *Appl. Energy* 2016, 163, 190–200.
- Ron Carter, S.B.; Thangavel, S. Regenerative Braking in PV-Mounted Electric Vehicle With Reduced Switch VSI-Driven BLDC Motor and HAP-FUP Controller. (Journal info missing).
- Pasupuleti, S.S.; Tummuru, N.R.; Misra, H. Power Management of Hybrid Energy Storage System Based Wireless Charging System with Regenerative Braking Capability. *IEEE Trans. Ind. Appl.* 2023, 59, 3785–3794.
- Fonseca de Freitas, C.A.; Bartholomeus, P.; Margueron, X.; Le Moigne, P. Series Architecture for the Reduction of the DC-DC Converter in a Hybrid Energy Storage System for Electric Vehicles. *Energies* 2023, 16, 7620.